

Exploiting Refrigerant Distribution for Predictive Control of Multi-Evaporator Vapor Compression Systems

Burns, D.J.; Bortoff, S.A.

TR2017-137 August 2017

Abstract

An observed behavior of refrigerant mass distribution in multi-path heat exchangers is exploited for control purposes. In this paper, we describe the following empirical property exploited for control: as the inlet valve position is decreased, refrigerant mass flow rate entering the heat exchanger is reduced, and for some flow rates, refrigerant is shown to preferentially flow in some paths more than others, causing maldistribution. This uneven refrigerant distribution is repeatable, reduces the capacity in a continuous manner and can be exploited with feedback controllers to regulate the perzone cooling. A controller is designed to provide stability and robustness to per-zone conditions and setpoints for this controller that relate per-path superheat temperature to overall evaporator capacity is created in such a way as to be robust to changes in local zone temperatures and the overall system evaporating temperature. This strategy provides zone decoupling and ultimately creates a virtual control input for a model predictive controller. Experiments demonstrate the effectiveness of this approach on a two-zone air conditioner in laboratory tests.

IEEE Conference on Control Technology and Applications (CCTA)

This work may not be copied or reproduced in whole or in part for any commercial purpose. Permission to copy in whole or in part without payment of fee is granted for nonprofit educational and research purposes provided that all such whole or partial copies include the following: a notice that such copying is by permission of Mitsubishi Electric Research Laboratories, Inc.; an acknowledgment of the authors and individual contributions to the work; and all applicable portions of the copyright notice. Copying, reproduction, or republishing for any other purpose shall require a license with payment of fee to Mitsubishi Electric Research Laboratories, Inc. All rights reserved.

Exploiting Refrigerant Distribution for Predictive Control of Multi-Evaporator Vapor Compression Systems

Daniel J. Burns[†] and Scott A. Bortoff

Abstract—An observed behavior of refrigerant mass distribution in multi-path heat exchangers is exploited for control purposes. In this paper, we describe the following empirical property exploited for control: as the inlet valve position is decreased, refrigerant mass flow rate entering the heat exchanger is reduced, and for some flow rates, refrigerant is shown to preferentially flow in some paths more than others, causing maldistribution. This uneven refrigerant distribution is repeatable, reduces the capacity in a continuous manner and can be exploited with feedback controllers to regulate the per-zone cooling.

A controller is designed to provide stability and robustness to per-zone conditions and setpoints for this controller that relate per-path superheat temperature to overall evaporator capacity is created in such a way as to be robust to changes in local zone temperatures and the overall system evaporating temperature. This strategy provides zone decoupling and ultimately creates a virtual control input for a model predictive controller. Experiments demonstrate the effectiveness of this approach on a two-zone air conditioner in laboratory tests.

I. INTRODUCTION

The structure and construction of vapor compression systems (VCS) used for comfort conditioning have evolved to increasing complexity since their initial commercialization more than 100 years ago. Vapor compression systems are now the most common means for commercial and residential space cooling [1], often employed for space or water heating [2], and extensively used in refrigeration (both stationary and mobile [3], [4]), desalination [5], [6], and cryogenic applications [7]. Recent advancements in power electronics, embedded computing and the commodification of electric motors have led to wide deployment of actuators with variable control authority such as inverter-driven compressors, variable speed fans and electronically-positioned expansion valves [8].

Additionally, market pressure has caused manufacturers to reduce the number of actuators and sensors where possible [9] in an effort to reduce costs. As a result of these trends, there are emerging opportunities for more advanced control of variable-actuation vapor compression systems, but these new strategies must conform to the restrictions imposed by a limited number of sensors and the valving/piping arrangement that meets performance expectations with the fewest number of machine components.

Multi-evaporator vapor compression systems (ME-VCS), such as those used in refrigeration systems and multi-room residential air conditioning applications, split refrigerant flow

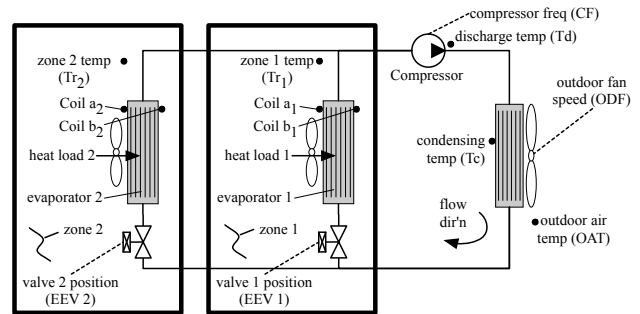


Fig. 1. Refrigerant piping arrangement of a multi-evaporator vapor compression system. Available sensors are shown as dots and control inputs are indicated with dashed lines.

among several heat exchangers to simultaneously provide cooling to multiple zones. Many studies on the control of multi-evaporator systems often include expansion valves on both the inlet and outlet sides of each evaporator, simplifying the control objectives as evaporator pressures become decoupled [10]. However, due to economic pressures previously mentioned, restriction valves on the exit side of each evaporator are often eliminated, resulting in the type of system shown in Fig. 1 (in particular, note the lack of valves at the outlet of either evaporator.). This parallel arrangement of valves in the refrigeration circuit results in a common evaporating pressure for all evaporators whose associated expansion valves are not closed. Although the expansion valves may be individually set to different openings, the overall high and low pressures are determined by the joint combination of the inlet valve openings. And since the evaporation process is isothermal when it is isobaric, all active evaporators are forced to operate at a single temperature. Therefore, the lack of valves at the outlet of each evaporator imposes a constant evaporating temperature for the entire multi-evaporator system.

While evaporators within the ME-VCS may be mutually coupled, the heat loads and desired zone air temperatures for each zone are not—the cooling required by each zone are independent. Therefore, a challenge ME-VCS controllers must address is how to modulate cooling for each evaporator in a coupled system given the independent zone thermal requirements. Typical control strategies employed in the literature modulate the capacities by operating the evaporators in a duty cycled fashion [11]. That is, despite using valves that are capable of variable apertures, many commercial systems use the valve as an ‘on-off’ style actuator. A consequence of this periodic opening and closing of expansion valves is the

D. J. Burns and S. A. Bortoff are with Mitsubishi Electric Research Laboratories, Cambridge, MA, Email: [burns, bortoff]@merl.com

[†] Corresponding author.

induced disturbances created in many internal temperatures and pressures within the machine.

Additionally, for equipment protection and efficient operation, a ME-VCS controller should enforce limits on pertinent machine temperatures and pressures. Model predictive control is an attractive approach for this problem [12], but duty cycling induces perturbations into these constrained outputs that are difficult to predict. Moreover, for the general case of an N -indoor unit system, $N - 1$ evaporators may be duty cycling with different periods that depend on the local zone conditions. Therefore, $N - 1$ large-amplitude disturbances, each with unpredictable periods are likely to induce perturbations into system outputs, precluding development of prediction models and therefore of model predictive controllers.

In order to smoothly and continuously modulate the cooling capacity of evaporators in a multi-evaporator vapor compression system, this paper reports an observed behavior of refrigerant mass distribution in multi-path heat exchangers and exploits this behavior for control purposes. This refrigerant distribution within a heat exchanger is repeatable, and although unstable with respect to small perturbations in local conditions, it can be stabilized with simple feedback and a low cost temperature sensor installed on each path. Using the method presented here, individual heat exchangers that are coupled through the pressure dynamics can be independently regulated to meet the local zone loading conditions without inducing perturbations, thereby enabling the subsequent development of model predictive control for equipment control.

The remainder of this paper is organized as follows: A physical description of the plant, the control objectives and corresponding predictive controller are described in Section II. The predictive controller relies on an observed property of refrigerant distribution in multi path heat exchangers that is described in Section III. Based on these observations, an inner loop controller is developed in Section IV, and its performance is experimentally characterized and compared to a duty cycling controller. Finally, experimental validation of the predictive controller is provided in Section V followed by concluding remarks.

II. CAPACITY CONTROL WITH SUPERVISORY MPC

This section briefly describes the multi-evaporator vapor compression system (ME-VCS) and outlines the design of a multivariable model predictive controller.

A. Physical Description

The ME-VCS (Fig. 1) is comprised of a single outdoor unit and N indoor units. When operating in cooling mode, the outdoor unit receives low pressure refrigerant in the vapor state from the indoor units. The compressor performs work to increase the refrigerant pressure and temperature, and the amount of work done is controlled by the compressor rotational frequency CF. A sensor measures the discharge temperature Td of the refrigerant leaving the compressor. The refrigerant then flows through the outdoor heat exchanger across which a fan forces air. This removes heat from the

refrigerant and causes it to condense and change phase from vapor to a saturated liquid. The amount of heat removed from the refrigerant depends on the outdoor air temperature OAT and outdoor fan speed ODF. In cooling mode, the outdoor unit heat exchanger acts as a condenser, and the phase change of the refrigerant in the condenser is assumed to be isobaric and occurs at a constant condensing temperature Tc which is measured by a sensor on the heat exchanger.

The ME-VCS has N indoor units indexed by $i \in \mathcal{I} = \{1, \dots, N\}$. High pressure liquid refrigerant from the outdoor unit is routed to the indoor units. The amount of refrigerant that enters the indoor unit is controlled by the opening position EEV _{i} of the electronic expansion valve, which is under the direction of the capacity controllers previously described. As the refrigerant flows through the expansion valve, it experiences a rapid drop in pressure and temperature and changes state into a two-phase mixture of liquid and vapor. The low temperature two-phase refrigerant then flows through the indoor unit heat exchanger. A fan forces air from the zone across the heat exchanger, which absorbs heat from the zone. For the system considered, zone occupants can directly specify fan speed for personal comfort, therefore we do not consider the fan speed as an input available to the controller. An unmeasured heat load acts in each zone. The heat absorbed by each indoor unit causes the refrigerant to evaporate from a two-phase mixture to a saturated vapor. The phase change is assumed to be isobaric and occurs at a constant evaporating temperature Te, which is measured by sensors on the indoor unit heat exchangers. Refrigerant is then routed back to the inlet of the compressor, completing the cycle.

The dynamics of the system that consists of the ME-VCS where the EEVs are controlled by the capacity controllers about a particular operating point is assumed to be linear. Accordingly, the dynamics of the N -zone ME-VCS are modeled by

$$x(t+1) = Ax(t) + Bu(t) \quad (1a)$$

$$w(t+1) = Iw(t) \quad (1b)$$

$$y(t) = Cx(t) + Iw(t) \quad (1c)$$

where the inputs $u = \text{col}(\text{CF}, \text{CC}_i) \in \mathbb{R}^{N+1}$, $i = 1, \dots, N$ are the compressor frequency CF and the capacity commands for each zone (which are further explained in Section IV, and the outputs $y = \text{col}(\text{Td}, \text{Te}, \text{Tc}, \text{Tr}_i) \in \mathbb{R}^{N+3}$ $i = 1, \dots, N$ are the discharge Td, evaporating Te, condensing Tc, and zone Tr _{i} temperatures. The model is fit to input-output data, and thus the states $x(t) \in \mathbb{R}^n$ are non-physical. The additive output disturbance $w(t) \in \mathbb{R}^{N+3}$ is used to capture the effects of outdoor air temperature OAT and zone heat loads on the measured outputs $y(t)$ for an offset-free estimator, and these disturbances are assumed constant over the timescale of the ME-VCS dynamics (1), which is a discrete time model sampled with a period of 1 min. The prediction horizon is chosen to be 30 min in order to capture the room dynamics.

The model (1) is experimentally identified at a typical operating condition and is a minimal realization of the

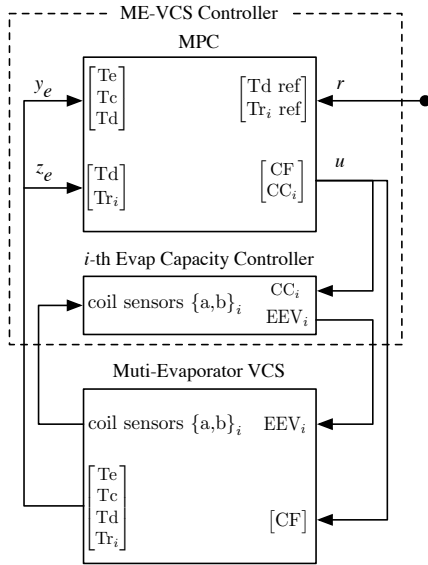


Fig. 2. Block diagram of the ME-VCS controller consisting of the capacity controllers for each evaporator coordinated by a model predictive controller.

dynamics. The pairs (A, B) and (A, C) are controllable and observable, respectively. The signals $u(t)$, $y(t)$, and $w(t)$ are the deviations of the inputs, outputs, and disturbances from their nominal values.

B. Model Predictive Controller

The control objective is to drive the zone temperatures to their respective setpoints in the presence of unmeasured heat loads and changes in outdoor air temperature, while enforcing constraints on critical system temperatures. To that end, a model predictive controller is formulated based on (1). Zone temperature errors $e_i = Tr_i - Tr_{i,ref}$ are created and penalized in a cost function, and a constrained optimal control problem is formulated. The optimal control problem is solved online in a receding horizon fashion and the first step in the sequence of control inputs from the solution is applied to the machine, as is customary in the model predictive control approach. For details of the MPC design of this system, see [12].

A block diagram of the control architecture is shown in Fig. 2. The overall ME-VCS controller consists of the model predictive controller and capacity controllers.

III. MULTI-PATH HEAT EXCHANGER

This section reports an empirical characteristic of refrigerant distribution in a multi-path heat exchanger as the associated expansion valve is changed. A commercially-available two-zone variable refrigerant flow (VRF) type air conditioner is installed in three adiabatic test chambers (one for each indoor unit and one for the outdoor unit). The air temperatures and heat loads in each test chamber are regulated by a secondary balance-of-plant system.

Refrigerant flow within the indoor unit heat exchangers are split among two paths as shown in Fig. 3A. Two temperature sensors (labeled points ‘a’ and ‘b’ in Fig. 3A)

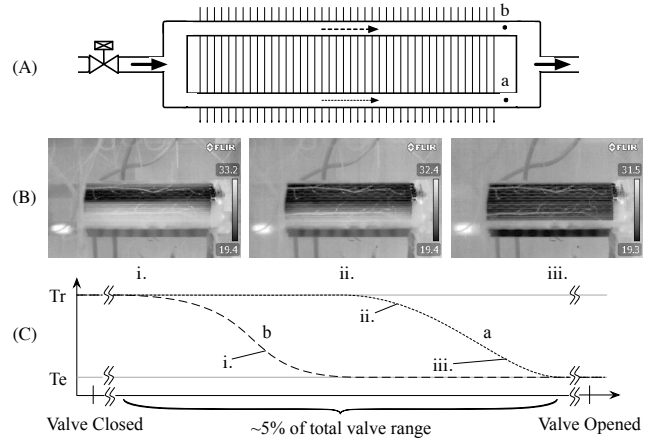


Fig. 3. (A) Multi-path heat exchanger with paths labeled ‘a’ and ‘b.’ (B) Infrared images of a multi-path heat exchanger for three different valve openings, i–iii. (C) Temperatures for paths a and b vary between the evaporating temperature Te and zone temperature Tr as the valve opening is changed. The three conditions represented by the IR images are indicated.

to measure the surface temperatures of the heat exchanger coil at some distance along each path.

Fig. 3B shows thermographic images of the heat exchanger as the expansion valve position is changed, and Fig. 3C is an illustration of the corresponding path temperatures. Starting from the valve fully opened, both paths are filled with mostly two-phase refrigerant and therefore both path temperatures are at the system evaporating temperature (right side of Fig. 3C). However, as the valve is closed, refrigerant in path a becomes superheated while path b remains at the evaporating temperature (labeled ‘iii’ in Fig. 3B and C). The valve is further reduced and more superheating occurs in path a (Fig. 3C-ii) until the temperature in that path of the coil warms to the zone temperature. Subsequent reduction in the valve opening causes superheating to occur in path b (Fig. 3C-i).

The observation that superheating for each path occurs at different operating conditions establishes that two-phase refrigerant preferentially flows along one path as the mass flow rate is reduced. As one and then both paths become superheated, a smaller fraction of the evaporator surface area is used for heat exchange. This is in contrast with typical strategies where the conditions at the evaporator outlet are controlled. In that approach, the conditions at the outlet can become superheated to the point where the refrigerant temperature reaches the air temperature, and that measurement is saturated and provides no additional information useful for control. This outlet saturation point can occur even though a substantial fraction of the refrigerant in the heat exchanger remains in two-phase, depending on the specific design and configuration of the heat exchanger. However, by controlling the per-path temperature with a single expansion valve as we propose, the ability to remove heat of the entire heat exchanger can be smoothly and continuously reduced over a greater range of cooling capacity (where cooling capacity is defined as the rate of thermal energy removed from the

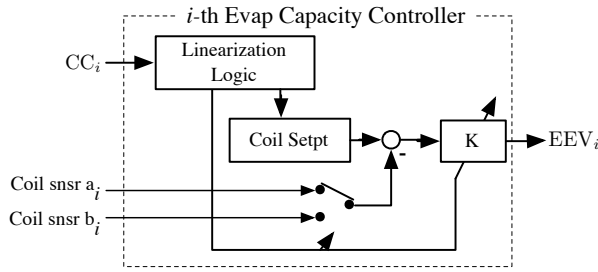


Fig. 4. Block diagram of the evaporator capacity controller used to control the refrigerant distribution in a multi-path heat exchanger and thereby modulate the cooling capacity.

zone by the evaporator per unit time and has units of Watts). Therefore, we expect an increased ability to regulate zone temperatures in the presence of widely differing heat loads.

Unfortunately, the range of valve openings over which the per-path temperatures change is narrow and sensitive to the operating conditions. Specifically, Fig. 3C shows a zoomed-in range of valve positions that provide sensible changes in path temperatures, where most of the range occurs with no sensible change in path temperatures (evaporator flooded or starved). For the systems tested, it is found that about 5% of the total valve operating range spans the heat exchanger operation from mostly two-phase to mostly superheated. But this narrow range of valve positions for which the path temperatures are controllable depend on the particular operation of the machine—*e.g.*, the refrigerant mass flow rate through the heat exchanger, the air flow rate, the operating pressures, the heat load, *etc.* Furthermore, the heat exchanger state is unstable: if the heat exchanger is operating such that one path is within the sensible range, then small changes in heat load will increase the heat transfer, causing more superheating, reducing the cooling capacity and ultimately leading to the saturation of one or both measurements. However, this phenomenon can be stabilized with feedback, enabling a smooth reduction in cooling capacity with capacity controller as described in the next section.

IV. CAPACITY CONTROL

Controlling the zone temperatures by directly manipulating the associated electronic expansion valve (EEV) emphasizes the nonlinear capacity relationship previously described, and in fact, most commercial systems treat the expansion valves as binary actuators and duty cycle them to control zone temperatures. In this section, we present a capacity controller that acts as an inner feedback loop to a supervisory controller, and compare our proposed capacity controller to the duty cycling method. Our capacity controller results in a linear, low-order transfer function from the capacity command signal to zone temperature that can subsequently be included in a linear model predictive controller.

The refrigerant distribution within a multi-path heat exchanger (and the corresponding reduction in cooling capacity) is exploited here to create cooling capacity controllers for each evaporator in a ME-VCS. The capacity controller

is designed to provide a continuous reduction in available capacity by manipulating the associated expansion valve EEV, such that a selected path temperature is driven to a setpoint. The coil setpoints are determined to relate the path superheat temperature to the desired reduction in cooling capacity. A block diagram of the capacity controller is shown in Fig. 4.

The controller receives a capacity command CC indicative of a desired capacity from a supervisory control system, expressed as a percentage of the maximum rated capacity. Using this capacity command, a function (labeled ‘Linearization Logic’ in Fig. 4) (i) selects the appropriate coil sensor to be used as the measured variable, (ii) provides the capacity command to a lookup table of coil setpoints, and (iii) modifies the parameters of a gain scheduled regulator.

The coil setpoint function codifies the observed relationship between coil path temperatures and different refrigerant distributions that lead to changes in cooling capacity. For the heat exchangers tested here, we have selected $CC \geq 50\%$ to be associated with coil sensor a , and $CC < 50\%$ to be associated with coil sensor b . The selection of 50% is somewhat arbitrary, but matches with the experimentally measured capacity when sensor a saturates. The lookup table relating per-path superheat temperatures to capacity reduction is similarly determined from experimental characterization, and errors in this lookup table are minimized through the robustness of feedback in the supervisory predictive controller as explained in Section II. Because the time constant in the transfer function from EEV to coil temperature can vary depending on which coil sensor is selected, we modify the feedback gains of the regulator to maintain acceptable transient performance. A feedback regulator K manipulates the EEV such that the selected coil temperature is driven to the corresponding setpoint value determined from the lookup table.

A. Capacity Control Linearizes the Zone Temp Response

The effect of the capacity controller is shown in a step response test in Fig. 5. The capacity controller previously described manipulates the EEV in zone 1 of a two-zone ME-VCS. Experimental conditions are chosen such that equilibrium is achieved at about 70% of the evaporator capacity, and all other ME-VCS actuators are held constant. At $t = 10$ min, the capacity command is increased stepwise to 90% (Fig. 5, top) and the resulting coil and zone temperature responses are recorded (Fig. 5, bottom).

As a result of the increased capacity command, the coil setpoint for path a is reduced from about 20°C to 16°C . The feedback regulator K opens the EEV (Fig. 5, EEV_1) driving the path temperature to this new coil setpoint. As a result, the overall cooling capacity of the evaporator is increased, which causes a reduction in the zone temperature (Fig. 5, Tr_1).

The architecture of the capacity controller uses feedback to drive the system to where the EEV retains control authority over capacity, and therefore control authority over the zone temperature. Therefore, the capacity controller enables the

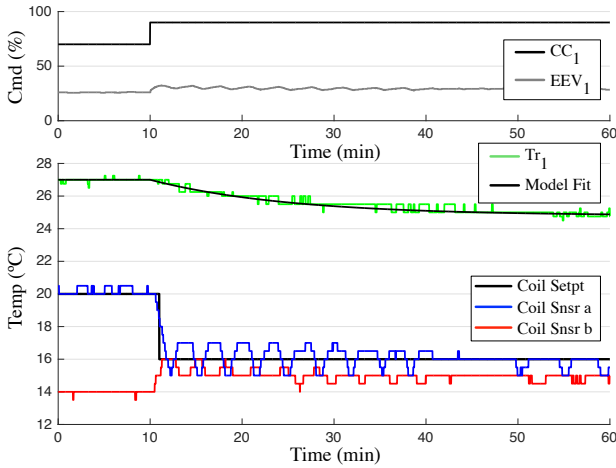


Fig. 5. A step change in capacity command results in a room temperature response to which a linear model is fit. Top: capacity command for zone 1 and the EEV position. Bottom: Coil setpoint for the selected heat exchanger path, and the two coil temperatures. The resulting zone temperature is also shown, as well as the response of a model fit to the transfer function from CC to Tr.

creation of a simple model from the capacity command signal CC to zone temperature Tr. The linearized dynamics for the i -th indoor unit when controlled by the capacity controller are modeled by

$$x_i(t+1) = A_{ii}x_i(t) + B_i u_i(t) \quad (2a)$$

$$y_i(t) = C_{ii}x_i(t) + w_i(t) \quad (2b)$$

for $i = 1, \dots, N$ for each of the N indoor units. The input $u_i = CC_i \in \mathbb{R}$ is the capacity command and the output $y_i = Tr_i \in \mathbb{R}$ is the zone temperature. The state of the i -th indoor unit $x_i \in \mathbb{R}^{n_i}$ is non-physical. The additive output disturbance $w_i(t)$ accounts for the unmeasured heat load on the zone temperature. The parameters of model (2) are fit to the data of Fig. 5, and the response of the resulting model is shown.

B. Comparison to Duty Cycling Control

This section presents experiments demonstrating that the capacity controllers enable a continuous and predictable reduction in cooling capacity when compared to a conventional duty cycling controller. The test conditions used for both control methods are as follows: the outdoor air temperature setpoint is 35°C , and the heat load setpoints are approximately 1400 W for both indoor zones. Additionally, the air temperature setpoints in zone 1 and 2 are 20°C and 25°C , respectively. The test conditions are chosen so that the zone setpoints are substantially different, and therefore require zone 2 to reduce its cooling capacity in order to regulate the air temperature to higher setpoints.

The results for the step increase in zone 2 are shown in Fig. 6. At $t = 10$ min, the zone setpoint is increased from 25°C to 27°C , which requires the respective methods to reduce the capacity in zone 2 while satisfying the requirements of zone 1. Additionally thermographic images at selected

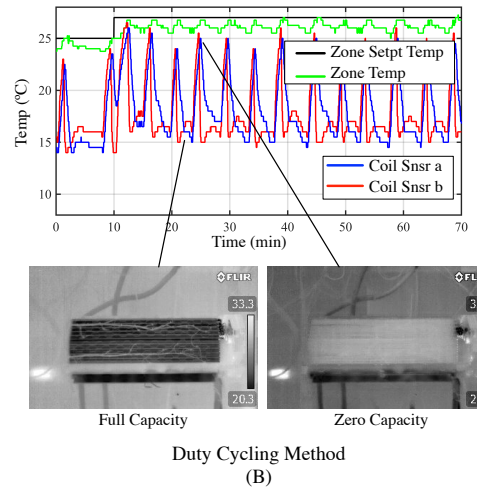
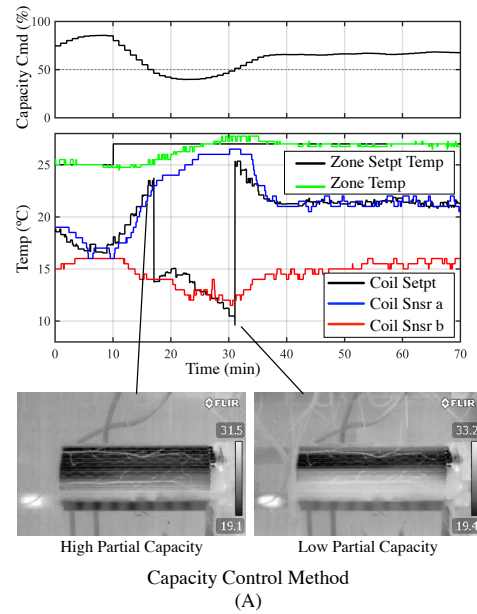


Fig. 6. (A) The capacity control method is used to reduce the capacity of a second evaporator in a ME-VCS in order to allow the zone temperature to increase. The capacity command is shown in top figure, and the resulting coil temperatures and zone temperature is shown in the middle figure. The bottom figures show two IR images of the heat exchanger at selected times from the transient showing partial capacity control. (B) The duty cycling method controls the EEV to periodically shut off the heat exchanger in an effort to warm the zone temperature.

times are shown below both figures to illustrate differences in heat exchanger utilization between the two methods.

For these test conditions, the initial steady state occurs with the heat exchanger at a relatively high cooling capacity (around 80%) as shown in Fig. 6A. At $t = 10$ min, the zone setpoint temperature is increased. The the capacity command (top plot) is reduced accordingly. As the capacity command is reduced between times $t = 10$ min and $t = 17$ min, the coil setpoint temperature is increased and the capacity controller manipulates the EEV such that coil sensor a (blue) follows the coil setpoint (black). The capacity controller is thus controlling the superheat in path a during this time, with path b containing two-phase refrigerant.

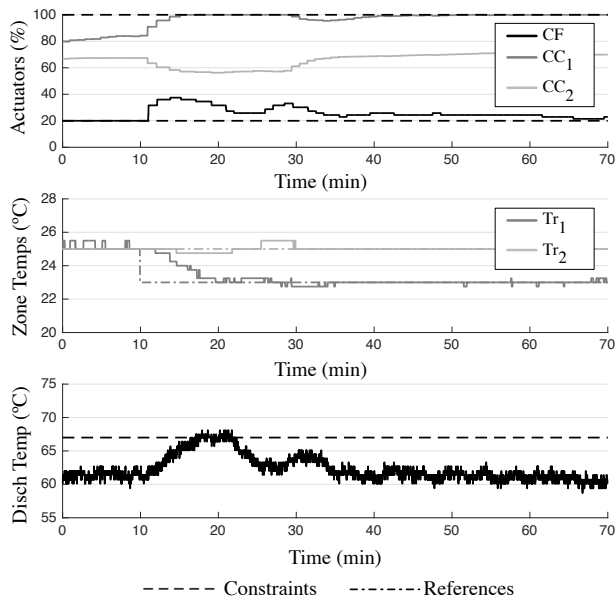


Fig. 7. Transient response using the capacity controller to drive zones to different setpoints. MPC selects inputs that simultaneously enforce constraints on CC input and Td output and results in zero steady state error in zone temperatures.

A similar experiment is conducted using the duty cycling method (Fig. 6B). In order to reduce the cooling capacity of zone 2, the duty cycling controller alternates the operation of the expansion valve from open (in which case two-phase refrigerant fills the evaporator shown in the thermographic image of Fig. 6B, left) to closed (in which case no refrigerant enters the heat exchanger which warms to the surrounding air temperature shown in the image of Fig. 6B, right).

Note that the duty cycling method induces oscillations in the zone temperature response. The period of these oscillations depend on the local thermodynamic conditions and controller tuning, and therefore are difficult to predict. In contrast, the capacity controller provides a smooth zone temperature response that is well approximated by the linear model (2). This model that includes the effect of capacity controllers on zone temperature is incorporated into a larger model of the entire machine dynamics in the next section, and is used as the basis for a model predictive controller.

V. PREDICTIVE CONTROLLER VALIDATION DATA

An experiment is performed to validate that model predictive control enforces constraints on a ME-VCS wherein the capacity controllers of Section IV are used to modulate evaporator capacity. A transient is induced wherein multiple constraints are simultaneously active (both input and output constraints) and the zones are driven to different temperatures with zero steady state error.

The test conditions are as follows: the outdoor air temperature setpoint is 35°C , and the heat loads are approximately 1400 W for both indoor zones. Additionally, the air temperature setpoints in both zones are set to 25°C . The system operates in closed loop using the model predictive controller.

The experimental results are shown in Fig. 7. Beginning from an equilibrium condition, a step change is applied to the setpoint in zone 1. The MPC selects CF, CC₁ and CC₂ commands to simultaneously drive zone 1 to its new setpoint, maintain zone 2 at its existing setpoint, and ensure that the discharge temperature remains below its upper bound. The experiment demonstrates that the capacity controllers are effective in modulating the evaporator capacities, independently controlling zone temperatures when coordinated by a model predictive controller that also enforces output constraints.

VI. CONCLUSIONS

This paper reports on refrigerant distribution in multi-path heat exchangers and its effect on capacity reduction. This property is exploited to develop capacity controllers that modulate the expansion valves in order to achieve a larger reduction in cooling capacities than otherwise obtained. The capacity controllers are then shown to linearize the response from capacity command to zone temperature, which is used to create a linear model predictive controller. Further studies are aimed at understanding the physical origin of the refrigerant distribution and extending the capacity control method to condensers in a multi-zone system operating in heating mode.

REFERENCES

- [1] K. J. Chua, S. K. Chou, and W. M. Yang, "Advances in heat pump systems: A review," *Applied Energy*, vol. 87, no. 12, Dec 2010.
- [2] A. Hepbasli and Y. Kalinci, "A review of heat pump water heating systems," *Renewable and Sustainable Energy Reviews*, vol. 13, no. 6–7, pp. 1211 – 1229, 2009.
- [3] M. Liu, W. Saman, and F. Bruno, "Development of a novel refrigeration system for refrigerated trucks incorporating phase change material," *Applied Energy*, vol. 92, pp. 336–342, APR 2012.
- [4] S. A. Tassou, G. De-Lille, and Y. T. Ge, "Food transport refrigeration—Approaches to reduce energy consumption and environmental impacts of road transport," *Applied Thermal Engineering*, vol. 29, no. 8–9, pp. 1467–1477, Jun 2009.
- [5] M. Hawlader, P. K. Dey, S. Diab, and C. Y. Chung, "Solar assisted heat pump desalination system," *Desalination*, vol. 168, no. 0, pp. 49 – 54, 2004.
- [6] V. Slesarenko, "Heat pumps as a source of heat energy for desalination of seawater," *Desalination*, vol. 139, no. 1–3, pp. 405 – 410, 2001.
- [7] J. Burger, H. Holland, E. Berenschot, J. Seppenwodde, M. ter Brake, H. Gardeniers, and M. Elwenspoek, "169 Kelvin cryogenic microcooler employing a condenser, evaporator, flow restriction and counterflow heat exchangers," in *14th IEEE International Conference On Micro Electro Mechanical Systems*, 2001, pp. 418–421.
- [8] J. Choi and Y. Kim, "Capacity modulation of an inverter-driven multi-air conditioner using electronic expansion valves," *Energy*, vol. 28, no. 2, pp. 141–155, FEB 2003.
- [9] A. R. Gopal, G. Leventis, A. Phadke, and S. d. I. R. du Can, "Self-financed efficiency incentives: case study of Mexico," *Energy Efficiency*, vol. 7, no. 5, pp. 865–877, OCT 2014.
- [10] M. S. Elliott and B. P. Rasmussen, "Decentralized model predictive control of a multi-evaporator air conditioning system," *Control Engineering Practice*, vol. 21, no. 12, SI, pp. 1665–1677, 2013.
- [11] B. Whitman, B. Johnson, and J. Tomczyk, *Refrigeration and Air Conditioning Technology*. Delmar, 1999.
- [12] D. J. Burns, C. Danielson, J. Zhou, and S. Di Cairano, "Reconfigurable model predictive control for multi-evaporator vapor compression systems," *IEEE Transactions on Control Systems Technology*, vol. PP, no. 99, pp. 1–17, 2017.